



Synergistic effects of graphene oxide and limestone calcined clay cement on mechanical properties and durability of concrete

Chava Venkatesh¹ · V. Mallikarjuna² · G. Mallikarjuna Rao³ · Santosh Kalyanrao Patil⁴ · B. Naga kiran⁵ · M. K. Yashwanth⁶ · C. Venkata Siva Rama Prasad⁷ · G. Sree Lakshmi Devi⁸

Received: 20 April 2024 / Revised: 18 June 2024 / Accepted: 28 June 2024
© The Author(s), under exclusive licence to Springer Nature Switzerland AG 2024

Abstract

This study investigates the synergistic effects of graphene oxide (GO) and limestone calcined clay cement (LC3) on the mechanical properties and durability of concrete. Various concrete mixes were prepared, including a reference mix, conventional concrete with 0.04% GO, and LC3 mixes with different clinker to calcined clay ratios (50:30, 45:35, and 40:40), both with and without GO. The mechanical properties were evaluated through compressive strength and split tensile strength tests, while durability was assessed using rapid chloride permeability, rapid chloride migration, water absorption, and corrosion rate measurements. The results revealed that the incorporation of GO in conventional concrete significantly improved both mechanical and durability properties. Among the LC3 mixes, the 45:35 clinker to calcined clay ratio exhibited the best performance. The combination of GO and LC3 resulted in remarkable enhancements, with the LC3 mix containing 0.04% GO and a 45:35 clinker to calcined clay ratio demonstrating the highest strength and durability performance. A strong positive correlation between compressive strength and split tensile strength was observed, and a power function equation was derived to predict split tensile strength based on compressive strength. The findings highlight the potential of combining GO and optimized LC3 for the development of sustainable and high-performance concrete with enhanced mechanical properties and durability.

Keywords Graphene oxide · Limestone calcined clay cement · Mechanical properties · Durability · Synergistic effects · Sustainable concrete

1 Introduction

Concrete, the world's most extensively utilized construction material, is projected to see a surge in production, reaching an astounding 18 billion tonnes annually by the middle of the 21st century [1, 2]. However, the manufacturing

of ordinary Portland cement (OPC), the essential binding agent in concrete, poses a significant environmental challenge, contributing to nearly 8% of the world's total CO₂ emissions [3]. In an effort to curb the ecological footprint of cement production and foster sustainable building practices, there is an increasing focus on developing innovative

✉ Chava Venkatesh
chvenky288@gmail.com

¹ Department of Civil Engineering, CVR College of Engineering, Vastunagar, Mangalpalli, Ibrahimpatnam, Telangana 501510, India

² Department of Civil Engineering, V. R. Siddhartha Engineering College, Vijayawada, India

³ Department of Civil Engineering, Chaitanya Bharathi Institute of Technology, Gandipet, Telangana, India

⁴ Department of Civil Engineering, K J College of Engineering and Management Research, Pune, Maharashtra 411048, India

⁵ Department of Civil Engineering, Rajeev Gandhi Memorial College of engineering and technology, Nandyal District, Andhra Pradesh, India

⁶ Department of Civil Engineering, Maharaja Institute of Technology Mysore, Mandya, Karnataka 571477, India

⁷ Department of Civil Engineering, Malla Reddy Engineering College, Secunderabad, Telangana 500100, India

⁸ Department of Civil Engineering, Nalla Malla Reddy Engineering College, Medchal District, Hyderabad, Telangana 500088, India

alternative binders and integrating cutting-edge materials into concrete compositions [4, 5].

Limestone calcined clay cement (LC3) has surfaced as a potential replacement for OPC, providing improved performance and reduced environmental impact [6, 7]. LC3 is produced by blending clinker with limestone and calcined clay, which are abundant and easily accessible materials [8]. The use of LC3 can significantly lower the clinker content in cement, leading to a decrease in CO₂ emissions related to cement production [9]. Furthermore, the pozzolanic reaction of calcined clay aids in the creation of additional hydration products, enhancing the “mechanical properties and durability of concrete” [10, 11].

Numerous studies have explored the performance of LC3 as an alternative to OPC. Scrivener et al. (2018) reported that LC3 can achieve comparable or superior compressive strength compared to OPC at both early and later ages, contingent on the composition and fineness of the materials [12]. Krishnan et al. (2019) also revealed that LC3 concrete exhibited enhanced compressive strength at 28 days compared to OPC concrete, with values spanning from 30 to 50 MPa [13]. The enhanced mechanical properties of LC3 concrete are due to the pozzolanic reaction of calcined clay, which produces more calcium silicate hydrate (C-S-H) gel, resulting in a more compact and uniform microstructure. [14, 15]. Similarly, several studies have also delved into the durability aspects of LC3 concrete; Maraghechi et al., (2018) Findings have shown that LC3 concrete with a clinker to calcined clay ratio of 50:30 demonstrated a 60% reduction in chloride ion penetration compared to OPC concrete at 28 days, with values ranging from 500 to 1000 coulombs [16]. Furthermore, LC3 concrete with the same clinker to calcined clay ratio exhibited a 45% reduction in carbonation depth compared to OPC concrete after 56 days of exposure, with values spanning from 5 to 10 mm [17]. The enhanced durability of LC3 concrete is attributed to the pozzolanic reaction of calcined clay, which refines the pore structure and forms additional hydration products like C-S-H and C-A-H, creating a denser, less permeable microstructure [18].

Recent progress in nanotechnology has enabled the creation of novel high-performance concrete materials [19]. One such material, graphene oxide (GO), a two-dimensional nanomaterial obtained from graphite, has attracted considerable interest owing to its exceptional thermal, mechanical, and electrical properties [20, 21]. Adding GO to cement-based materials have been demonstrated to improve the mechanical strength, fracture toughness, and durability of concrete [22, 23]. GO's distinctive features, including its large specific surface area and outstanding dispersibility in water, render it a perfect choice for use as a nano-reinforcement in concrete [24].

S.C. Devi et al. (202) have demonstrated the efficacy of GO in improving the mechanical properties of cement composites and concrete. For instance, her research has shown that incorporating a small percentage of GO by weight of cement can lead to significant increases in the 28-day compressive strength of cement composites, with values reaching 60–70 MPa [25]. Similarly, the addition of GO has been found to enhance the compressive strength of strain-hardening cementitious composites and cement mortar, with improvements ranging from 24.8 to 38.9% at 28 days [26, 27]. These enhancements in mechanical properties are attributed to the ability of GO to refine the microstructure, fill micro-cracks, and enhance the interfacial bonding between the cement matrix and the reinforcing materials [28].

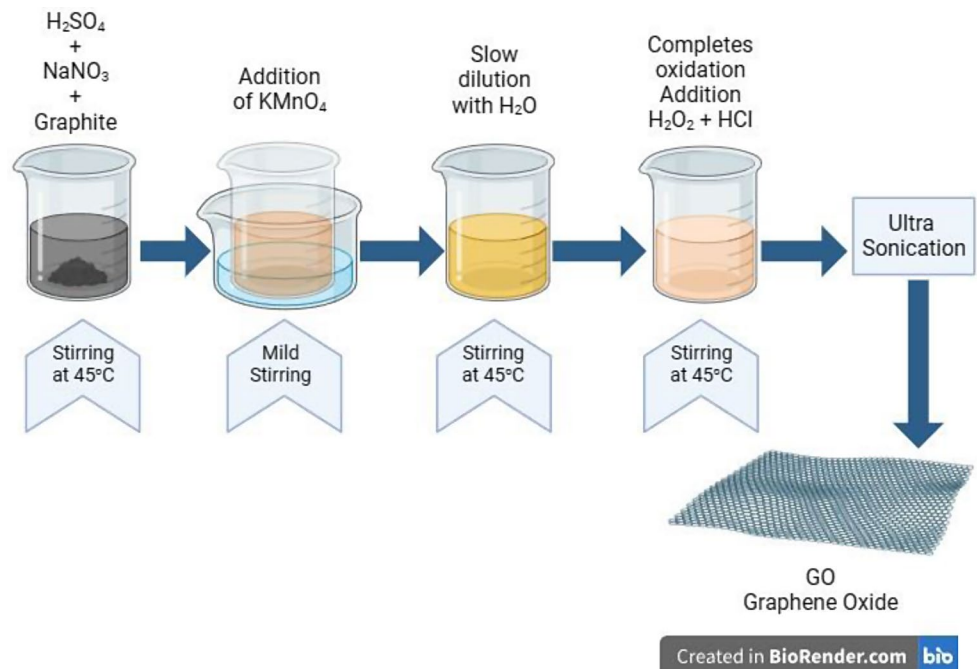
The durability aspects of GO-modified concrete have also been investigated, focusing on its resistance to “chloride ion penetration, water absorption, and freeze-thaw cycles”. Studies have reported that incorporating GO can result in significant reductions in chloride ion penetration and water absorption compared to plain cement concrete. For example, Mohammed et al. (2015) research has shown that adding 0.04% of GO by weight of cement can lead to a 45% decrease in chloride ion penetration and a 28% decrease in water absorption at 28 days [29]. The improved durability of GO-modified concrete is attributed to the ability of GO to fill micro-cracks, refine the pore structure, and improve the interfacial bonding between the cement matrix and the aggregates, resulting in a more compact and less permeable microstructure [30]. These results underscore the promise of GO as an innovative nanomaterial for creating high-performance and long-lasting concrete. Adding GO to concrete mixtures can substantially enhance mechanical strength and durability, paving the way for sustainable and enduring construction materials [31, 32].

Combining limestone calcined clay cement (LC3) and graphene oxide (GO) in concrete mixtures provides a promising path for creating environmentally friendly and high-performance construction materials. However, the potential synergistic effects of these materials on the “mechanical properties and durability of concrete” have not been thoroughly explored. Prior research has largely focused on the individual impacts of either LC3 [33, 34] or GO [35, 36] on the characteristics of concrete, leaving a gap in understanding their combined influence. To fully harness the potential of this innovative combination, a comprehensive investigation is necessary to elucidate the interplay between LC3 and GO and their effects on various performance indicators, such as “compressive strength, tensile strength, and durability metrics”. By unraveling the synergistic mechanisms at work, this research direction holds promise for the development of advanced concrete formulations that excel in both

Table 1 Chemical characteristics (weight%) and physical characteristics of binders

	CaO	Al ₂ O ₃	SiO ₂	Fe ₂ O ₃	K ₂ O	SO ₃	TiO ₂	Na ₂ O	LOI	Sg [#]	SSA(m ² /kg)*
OPC	64.28	5.06	18.76	4.76	0.38	1.43	0.56	0.71	4.06	3.12	405
Clinker	62.10	4.83	19.32	3.84	0.27	0.68	0.16	0.24	8.56	3.19	350
Calcined clay	1.10	22.75	59.67	4.73	0.32	0.02	1.64	0.10	9.67	2.50	920
Limestone	50.12	1.52	11.07	1.87	0.15	0.02	0.42	0.05	34.78	2.56	660

*SSA: Specific surface area, #Sg: Specific gravity

Fig. 1 Preparation of graphene oxide

sustainability and performance, paving the way for a new era of green and resilient construction materials.

Research Novelty: This study introduces a novel approach by investigating the synergistic effects of graphene oxide (GO) incorporation into Limestone Calcined Clay Cement (LC3) mixes, exploring various clinker to calcined clay ratios. Unlike previous research focusing solely on LC3 or GO in isolation, this study comprehensively evaluates the mechanical properties and durability of concrete, including “compressive strength, split tensile strength, chloride permeability, chloride migration coefficient, water absorption, and corrosion rate of steel reinforcement”. Furthermore, it employs regression analysis to establish predictive models for the relationship between “split tensile strength and compressive strength”, offering valuable insights into concrete performance. The optimization of LC3 mixes alongside GO integration promises to yield sustainable and high-performance concrete formulations, thus addressing environmental concerns while advancing construction material design. This research expands the existing knowledge base on sustainable construction materials, providing practical guidance for the development and application of advanced concrete mixtures in real-world construction scenarios.

2 Materials and methods

2.1 Materials

The OPC used conformed to the requirements of IS 12,269 – 2013 [37], which specifies the chemical and physical properties of 53 grade OPC, as shown in Table 1. LC3 was prepared by blending clinker with limestone and calcined clay in varying proportions. Three different clinker-to-calcined clay ratios were used: 50:30, 45:35, and 40:40. The limestone and calcined clay were obtained from local mines and ground to a fineness similar to that of OPC. The chemical composition of OPC and the raw ingredients/binders of LC3 was determined using “X-ray fluorescence (XRF) spectroscopy”. The samples were finely ground and pressed into pellets before being subjected to XRF analysis, their outputs are listed in Table 1. The results provided insights into the major and minor oxides present in the binders, which influence their hydration behavior and performance. The GO used in this study had a purity of 99% and was prepared using the Hummers method [38], as shown in Fig. 1. Elemental analysis revealed that GO consists of 51% Carbon (C), 45% oxygen, 1.5% hydrogen, 1% nitrogen, and

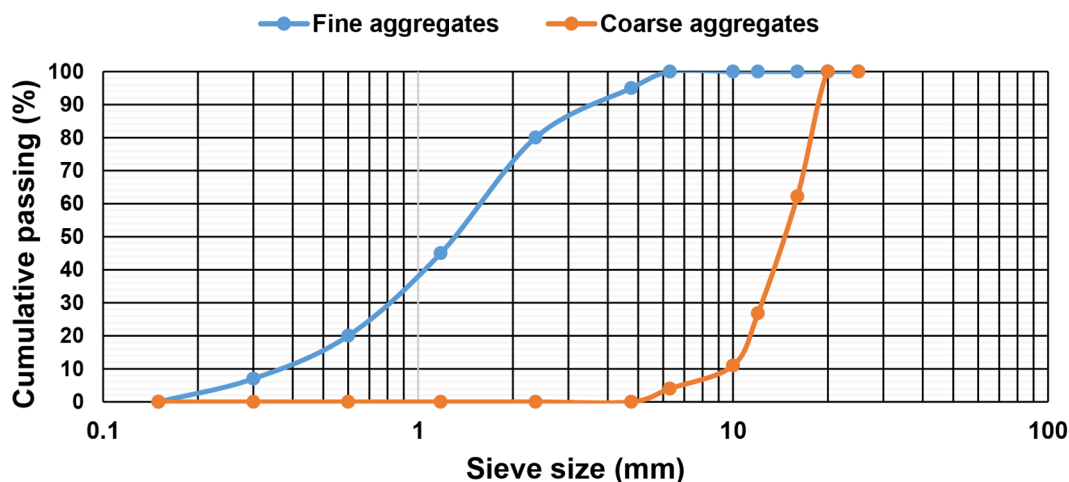


Fig. 2 Gradation curve for aggregates

Table 2 Physical properties of aggregates

Materials properties	Aggregates	
	Fine	Coarse
Specific gravity	2.66	2.74
Water absorption (%)	1.11	0.60
Fineness modulus	2.56	7.35
Bulk density	1.46	1.51

1.5% sulfur. In accordance with 383–2016 [39], the physical properties of both fine and coarse aggregates, including gradation, moisture content, and bulk density, were evaluated to verify their conformity with the applicable standards, as depicted in Fig. 2; Table 2.

2.2 Methods

2.2.1 Mix proportions and specimen preparation

Following IS 10,262–2019 [40], mix proportions were designed to reach a target compressive strength of 38.25 MPa at 28 days, as specified in Table 3. The water-to-binder ratio was maintained at 0.45, and the total binder content was kept constant at 450 kg/m³ for all mixtures. Adjustments to fine and coarse aggregate contents were made to maintain a consistent volume fraction, ensuring a workable and

cohesive concrete mix. Concrete specimens were prepared following “ASTM C192/C192M-19” guidelines [41]. Raw materials were accurately weighed and mixed in a 50-liter laboratory pan mixer. Dry ingredients were initially blended for 2 min, followed by the addition of water and GO (for mixes M1, M5, M6, and M7). Mixing continued for 3 min to ensure homogeneity. Freshly mixed concrete was poured into molds for testing. “Cubic molds (150 mm × 150 mm × 150 mm) were used for compressive strength, cylindrical molds (diameter 150 mm, height 300 mm) for split tensile strength, and disk molds (100 mm diameter, 50 mm thickness) for durability tests”. The concrete was placed in three layers and consolidated using a vibrating table. The specimens were covered with plastic sheets and cured for 24 h at ambient temperature. Subsequently, they were immersed in a water curing tank maintained at 27 ± 2 °C until the required testing age (3, 7, or 28 days) to ensure proper hydration and strength development [42]. A total of 504 samples were produced and tested.

2.3 Test methods

The compressive strength was assessed using ASTM C39/C39M-20 [43], where concrete cubes were subjected to

Table 3 Mix calculations (kg/m³)

Mix detailing	Mix designation	OPC	LC3				Aggregates		Water (liters)	GO
			Clinker	Calcined clay	Limestone	Gypsum	Fine	Coarse		
Conventional concrete (CC)	Ref.	450	---	---	---	---	624	1220	186	---
CC + 0.04% GO	M1	450	---	---	---	---	624	1220	186	18
LC3 50:30	M2	450	225	135	67.5	22.5	624	1220	186	---
LC3 45:35	M3	450	202.5	157.5	67.5	22.5	624	1220	186	---
LC3 40:40	M4	450	180	180	67.5	22.5	624	1220	186	---
LC3 50:30 + 0.04%GO	M5	450	225	135	67.5	22.5	624	1220	186	18
LC3 50:35 + 0.04%GO	M6	450	202.5	157.5	67.5	22.5	624	1220	186	18
LC3 40:40 + 0.04%GO	M7	450	180	180	67.5	22.5	624	1220	186	18

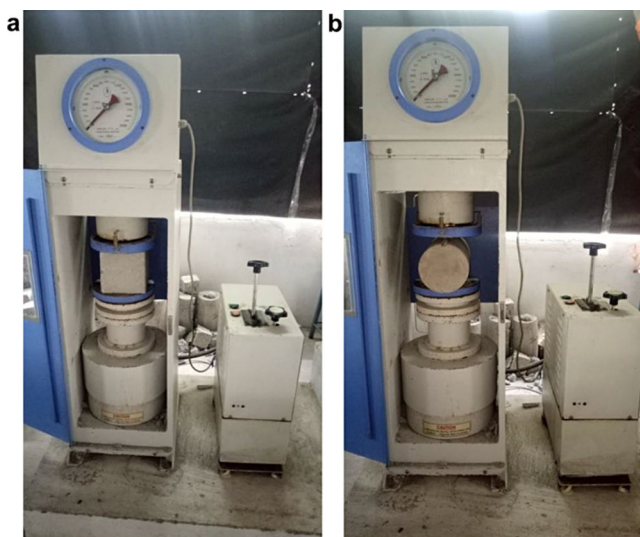


Fig. 3 (a) Experimental photograph of compressive strength test setup. (b) Experimental photograph of Split tensile strength test setup

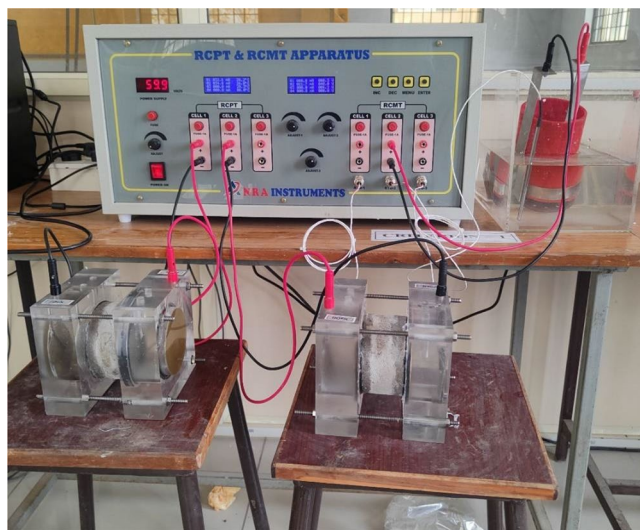


Fig. 4 Experimental setup for RCPT & RCMT

a constant loading rate of 0.25 MPa/s until failure. Split tensile strength was determined following ASTM C496/C496M-17 [44], with cylindrical specimens exposed to a diametral compressive load until failure. Resistance to chloride ion penetration was evaluated using two methods: The “Rapid Chloride Permeability Test (RCPT) as per ASTM C1202-19” [45], measuring the total charge passed through the specimen over a 6-hour period, and the “Rapid Chloride Migration Test (RCMT) according to NT BUILD 492” [46], determining the depth of chloride penetration using a colorimetric method. Water absorption was assessed using the sorptivity test (“ASTM C1585-13”) [47], where the rate of water absorption was determined by measuring mass gain over time. The corrosion rate of steel reinforcement was evaluated using the linear polarization resistance (LPR)

technique (ASTM G59-97(2020)) [48], employing a three-electrode system to measure polarization resistance and calculate corrosion current density. To gain insights into the significance of factors influencing the properties of the concrete mixes, statistical analysis, including “analysis of variance (ANOVA) and regression analysis”, was conducted [49]. ANOVA was used to evaluate the impact of GO and LC3 on various mechanical and durability properties, while regression analysis was employed to establish correlations between “compressive strength and split tensile strength”. Figures 3–7 depicts the experimental photographs of the above listed test methods.

3 Results and discussion

3.1 Compressive strength

Figure 8 illustrates the compressive strength progression of the different concrete mixtures at 3, 7, and 28 days. The mixes comprise the reference mix (M0), conventional concrete with 1% graphene oxide (GO) (M1), and limestone calcined clay cement (LC3) mixes with different clinker to calcined clay ratios, both with and without GO incorporation. The addition of GO in conventional concrete (M1) led to a notable enhancement in compressive strength compared to the reference mix (M0) at all ages. At 28 days, the compressive strength of M1 reached 45.38 MPa, surpassing that of M0 (41.12 MPa) by 10.35%. The enhancement can be attributed to the unique features of GO, such as its large specific surface area and outstanding mechanical properties, which facilitate the formation of a denser microstructure and stronger bonding between the cement matrix and aggregates [50, 51].

Among the LC3 mixes without GO (M2, M3, and M4), M3 with a 45:35 clinker to calcined clay ratio demonstrated the highest compressive strength at all ages. The 28-day compressive strength of M3 reached 44.37 MPa, surpassing that of M2 (50:30 ratio) and M4 (40:40 ratio) by 4.69% and 10.48%, respectively. This finding suggests the presence of an optimal clinker to calcined clay ratio for achieving enhanced mechanical properties in LC3 concrete [6]. The synergistic effect of combining GO with LC3 was evident from the improved compressive strength of LC3 mixes containing 1% GO (M5, M6, and M7) compared to their corresponding LC3 mixes without GO. The 28-day compressive strength of M6 (LC3 with a 45:35 clinker to calcined clay ratio and 1% GO) reached 52.39 MPa, exceeding the reference mix (M0) by 27.40% and the conventional concrete with 1% GO (M1) by 15.44%. This remarkable improvement underscores the potential of optimizing LC3 mixes

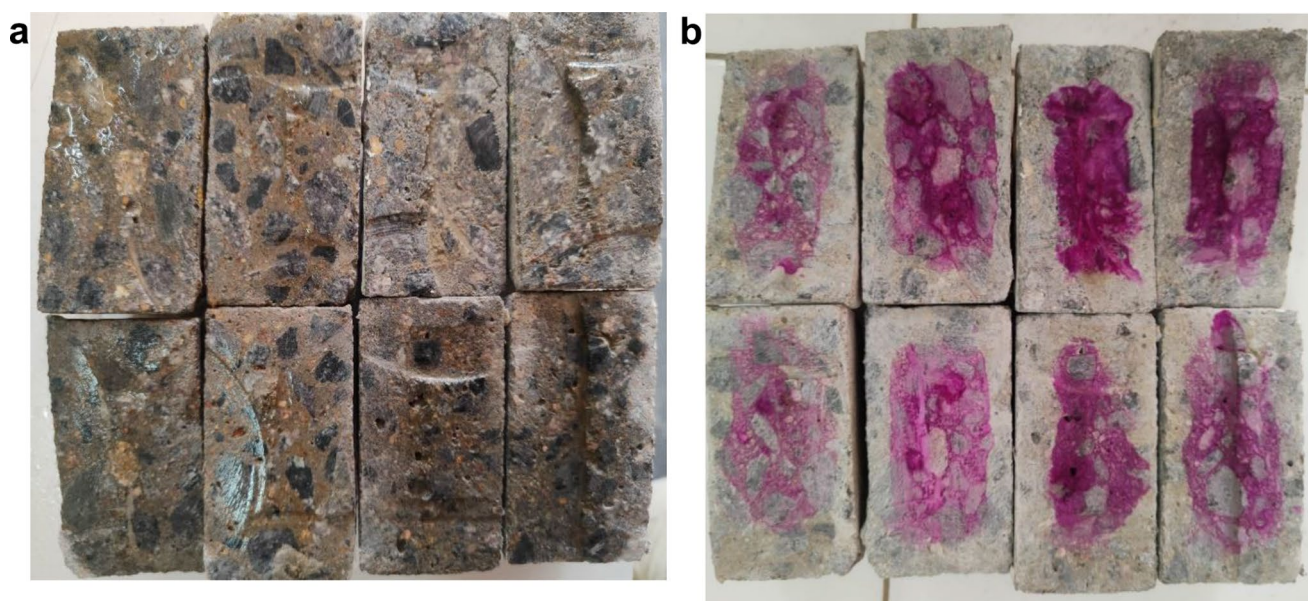


Fig. 5 (a) Silver nitrate sprayed on the specimens after RCMT test. (b) chloride ions penetration measurement by colorimetric method



Fig. 6 Experimental photo graph of sorptivity test

with GO addition to achieve superior mechanical properties [26] & [52].

The compressive strength development of all mixes exhibited a similar trend, with a rapid increase in early ages (3 and 7 days) followed by a more gradual increase up to 28 days. This behavior aligns with the hydration kinetics of cement-based materials, where the majority of strength gain occurs in the initial stages [53]. The outcomes of this study align with prior research on the application of GO in cement-based materials [30] & [53]. Previous studies have shown that adding GO improves the mechanical properties of concrete through several mechanisms, including filling micro-cracks, accelerating hydration reactions, and enhancing the interfacial



Fig. 7 Accelerated corrosion test setup

transition zone (ITZ) between the cement paste and aggregates [54].

3.2 Split tensile strength

Figure 9 presents the split tensile strength results of various concrete mixes at 3, 7, and 28 days. The incorporation of 1% GO in conventional concrete (M1) resulted in a substantial increase in split tensile strength compared to the reference mix (M0) at all ages. At 28 days, the split tensile strength of M1 reached 4.41 MPa, surpassing that of M0 (3.52 MPa) by 25.28%. This enhancement can be ascribed to the ability of GO to improve the tensile capacity of the cement matrix through crack bridging and stress transfer mechanisms [36] & [55]. Among the LC3 mixes

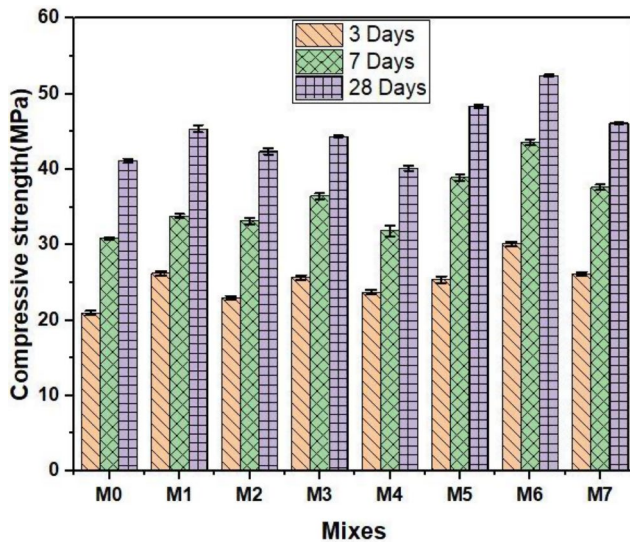


Fig. 8 Compressive strength test results

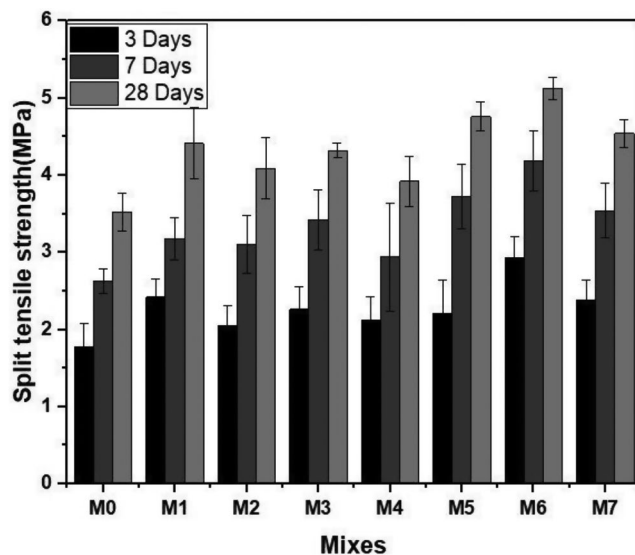


Fig. 9 Split tensile strength test results

without GO (M2, M3, and M4), M3 with a 45:35 clinker to calcined clay ratio exhibited the highest split tensile strength at all ages. The 28-day split tensile strength of M3 reached 4.32 MPa, exceeding that of M2 (50:30 ratio) and M4 (40:40 ratio) by 5.63% and 10.20%, respectively. This finding suggests that the optimal clinker to calcined clay ratio identified for compressive strength also favors the development of tensile strength in LC3 concrete [56].

The incorporation of 1% GO to LC3 mixes (M5, M6, and M7) led to a remarkable enrichment in split tensile strength compared to their corresponding LC3 mixes without GO. The 28-day split tensile strength of M6 (LC3 with a 45:35 clinker to calcined clay ratio and 1% GO) reached 5.12 MPa, surpassing the reference mix (M0)

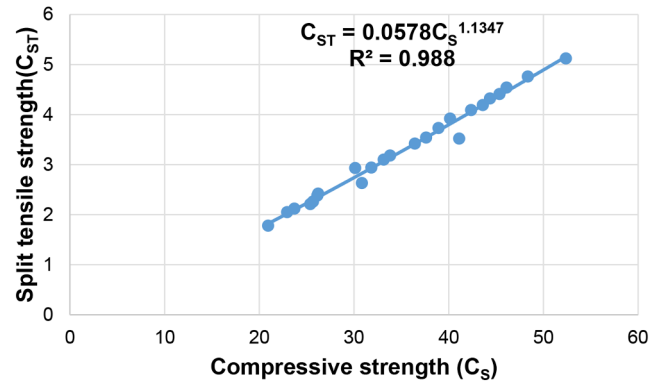


Fig. 10 co-relation between the compressive strength and split tensile strength

by 45.45% and the conventional concrete with 1% GO (M1) by 16.09%. This exceptional improvement highlights the synergistic effect of combining GO with LC3, where GO's ability to enhance tensile capacity complements the refined pore structure and improved interfacial bonding provided by the optimized LC3 system [25–27]. All mixtures displayed a split tensile strength development pattern resembling that of compressive strength, characterized by a swift increase at early ages (3 and 7 days) followed by a more gradual rise up to 28 days. This behavior aligns with the strength gain characteristics of cement-based materials, where the majority of tensile strength development occurs in the initial stages [57]. The results of this study align with prior research on the application of GO in cement-based materials, which has demonstrated notable enhancements in tensile strength [25] & [26]. The mechanisms behind the enhanced tensile capacity of GO-modified concrete include the ability of GO to arrest and deflect micro-cracks, distribute stress uniformly, and improve the interfacial bonding between the cement matrix and aggregates [54].

3.3 Correlation between the compressive strength and split tensile strength

Figure 10 illustrates the relationship between the “compressive strength and split tensile strength” of the different concrete mixtures at various ages (3, 7, and 28 days). The linear regression analysis indicates a robust positive relationship between the two mechanical properties, with a coefficient of determination (R^2) of 0.988. This suggests that approximately 98% of the variability in split tensile strength can be ascribed to the compressive strength of the concrete mixes [58].

The “relationship between compressive strength (CS) and split tensile strength (CST)” can be expressed by a power function equation, as shown in Eq. 1. This

Table 4 Predication of split tensile strength

Mixes	Experimental values						Predicted values		
	Compressive strength			Split tensile strength			$C_{ST}=0.0578C_S^{1.1347}$		
	3days	7days	28days	3days	7days	28days	3days	7days	28days
M0	20.94	0.298	30.84	1.78	0.298	2.63	1.82	2.83	3.92
M1	26.22	0.235	33.82	2.42	0.235	3.18	2.35	3.14	4.39
M2	22.95	0.256	33.15	2.05	0.256	3.1	2.02	3.07	4.06
M3	25.68	0.291	36.44	2.26	0.291	3.42	2.30	3.42	4.27
M4	23.71	0.305	31.84	2.12	0.305	2.94	2.10	2.93	3.82
M5	25.39	0.425	38.93	2.21	0.425	3.73	2.27	3.68	4.71
M6	30.14	0.281	43.61	2.93	0.281	4.19	2.76	4.19	5.16
M7	26.14	0.262	37.62	2.38	0.262	3.54	2.35	3.54	4.47

equation indicates that the split tensile strength increases non-linearly with increasing compressive strength, aligning with the findings of previous studies on the relationship between these two mechanical properties in concrete [59, 60].

$$C_{ST} = 0.0578(C_S^{1.1347}) \tag{1}$$

The experimental and predicted values of split tensile strength for the different concrete mixtures at various ages are shown in Table 4. The power function equation derived from the compressive strength results was used to calculate the predicted values. The comparison between the experimental and predicted values reveals a good agreement, with relatively small deviations. The mean absolute percentage error (MAPE) between the experimental and predicted values is 5.6%, indicating the reliability of the derived equation in estimating the split tensile strength from the compressive strength of the concrete mixes. The high R² value of 0.988 further confirms the accuracy of the prediction, indicating a strong relationship between the experimental and predicted split tensile strength values. This robust correlation supports the application of the power function equation as a dependable method for predicting the split tensile strength of concrete mixtures based on their compressive strength, within the scope of the investigated parameters [60].

The results underscore the importance of considering the “relationship between compressive strength and split tensile strength” in the design and evaluation of concrete mixes, particularly when incorporating novel materials such as GO and LC3. The ability to predict the split tensile strength from the compressive strength can facilitate the optimization of mix designs and the assessment of the potential benefits of incorporating these materials in terms of mechanical performance. By leveraging this relationship, researchers and engineers can streamline the development of high-performance concrete mixes that exhibit enhanced mechanical properties, ultimately

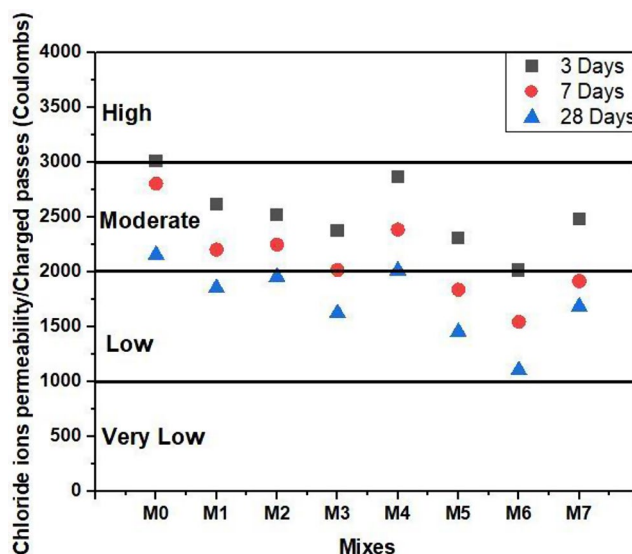


Fig. 11 Rapid chloride permeability test results

contributing to the advancement of sustainable construction practices.

3.4 Rapid chloride permeability test

Figure 11 displays the Rapid Chloride Permeability Test (RCPT) results for the different concrete mixtures. These findings provide important information about the resistance of the studied concrete mixtures to chloride ion penetration, which is a critical factor affecting the durability of concrete structures in environments with high chloride content [61]. Adding 1% GO to conventional concrete (M1) led to a significant decrease in the charge passed compared to the reference mix (M0), suggesting an enhancement in the resistance to chloride penetration. The charge passed for M1 was 1853 coulombs, which is 16.35% lower than that of M0 (2156 coulombs). The improvement can be attributed to GO’s capability to refine the pore structure of the cement matrix and enhance the interfacial bonding between the cement

paste and aggregates, consequently decreasing the permeability of the concrete [29].

Among the LC3 mixes without GO (M2, M3, and M4), M3 with a 45:35 clinker to calcined clay ratio demonstrated the lowest charge passed (1623 coulombs), which is 32.8% lower than that of the reference mix (M0). The enhanced resistance to chloride penetration can be ascribed to the pozzolanic reaction of the calcined clay, which results in the creation of supplementary hydration products that make the microstructure denser and decrease the porosity of the cement matrix [62]. The synergistic effect of combining GO and LC3 is evident from the substantial reduction in the charge passed for LC3 mixes containing 1% GO (M5, M6, and M7) compared to their corresponding LC3 mixes without GO. Mix M6 (LC3 with a 45:35 clinker to calcined clay ratio and 1% GO) exhibited the lowest charge passed among all the investigated mixes, with a value of 1103 coulombs, which is 95.46% lower than that of the reference mix (M0) and 67.99% lower than that of the conventional concrete with 1% GO (M1). This remarkable improvement highlights the combined benefits of GO and LC3 in enhancing the chloride penetration resistance of concrete.

The RCPT results can be categorized according to the ASTM C1202 classification [45], which rates the chloride ion penetrability of concrete based on the charge passed. The reference mix (M0) and conventional concrete with 1% GO (M1) fall under the “low” penetrability class, while all the LC3 mixes, both with and without GO, belong to the “very low” penetrability class. This classification underscores the superior performance of LC3-based concrete mixes in resisting chloride ion penetration, which is further enhanced by the addition of GO [24].

The incorporation of GO and LC3 in concrete mixes has proven to be an effective strategy for enhancing the chloride

penetration resistance, a critical aspect of concrete durability. The synergistic effect of these materials can be attributed to their ability to refine the pore structure, densify the microstructure, and improve the interfacial bonding within the cement matrix. By optimizing the clinker to calcined clay ratio and incorporating GO, it is possible to develop high-performance concrete mixes with exceptional resistance to chloride ion penetration, ultimately leading to more durable and sustainable concrete structures in chloride-laden environments.

3.5 Rapid chloride migration test

Figure 12 depicts the rapid migration coefficients of chloride ions in various concrete mixes, including the reference mix (M0), normal concrete with 1% graphene oxide (GO) (M1), and limestone calcined clay cement (LC3) mixes with varying clinker to calcined clay ratios, both with and without GO addition. The rapid migration coefficient is an essential parameter for evaluating the resistance of concrete to chloride ion penetration, a key factor in determining the durability of reinforced concrete structures in environments with high chloride levels [18].

Incorporating 1% GO in conventional concrete (M1) led to a significant reduction in the rapid migration coefficient compared to the reference mix (M0). The rapid migration coefficient of M1 was $6.5 \times 10^{-12} \text{ m}^2/\text{s}$, which is 37.84% lower than that of M0 ($8.96 \times 10^{-12} \text{ m}^2/\text{s}$). This enhancement can be attributed to GO's ability to refine the pore structure of the cement matrix, reducing the connectivity of capillary pores and increasing the tortuosity of the pore network, thus impeding the migration of chloride ions [22, 63].

Among the LC3 mixes without GO (M2, M3, and M4), M3 with a 45:35 clinker to calcined clay ratio demonstrated the lowest rapid migration coefficient ($7.1 \times 10^{-12} \text{ m}^2/\text{s}$), which is 26.17% lower than that of the reference mix (M0). The decrease in chloride ion migration can be ascribed to the pozzolanic reaction of the calcined clay, which leads to the creation of supplementary hydration products that make the microstructure denser and reduce the porosity of the cement matrix, consequently improving the resistance to chloride ion penetration [5, 6].

The synergistic effect of combining GO and LC3 is evident from the significant reduction in the rapid migration coefficients of LC3 mixes containing 1% GO (M5, M6, and M7) compared to their corresponding LC3 mixes without GO. Mix M6 (LC3 with a 45:35 clinker to calcined clay ratio and 1% GO) exhibited the lowest rapid migration coefficient among all the investigated mixes, with a value of $2.86 \times 10^{-12} \text{ m}^2/\text{s}$, which is 65.0% lower than that of the reference mix (M0) and 127.97% lower than that of the normal concrete with 1% GO (M1). The significant decrease in

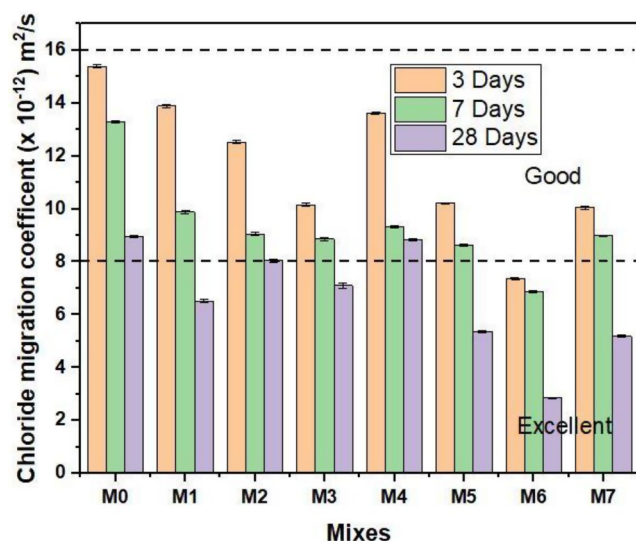


Fig. 12 Rapid migration coefficients of LC3

chloride ion migration underscores the synergistic advantages of combining GO and LC3 to enhance the durability of concrete.

The decrease in rapid migration coefficients of the LC3 mixtures containing GO can be ascribed to the synergistic effects of GO and calcined clay on the microstructure of the cement matrix. GO contributes to refining the pore structure, decreasing the connectivity of capillary pores, and increasing the tortuosity of the pore network. Simultaneously, the pozzolanic reaction of calcined clay results in the creation of supplementary hydration products that further densify the microstructure [64]. This synergistic action produces a denser and less permeable cement matrix, which effectively impedes the migration of chloride ions.

3.6 Sorptivity

Figure 13 showcases the sorptivity coefficients of various concrete mixes, including the reference mix (M0), normal concrete with 1% graphene oxide (GO) (M1), and limestone calcined clay cement (LC3) mixes with varying clinker to calcined clay ratios, both with and without GO addition. Sorptivity is a vital parameter that characterizes the capillary water absorption behavior of concrete, which is closely related to its durability performance, particularly in terms of resistance to water and chloride ingress [65].

The inclusion of 1% GO in normal concrete (M1) led to a substantial decrease in the sorptivity coefficient compared to the reference mix (M0). The sorptivity coefficient of M1 was 0.51 mm/min^{0.5}, which is 21.56% lower than that of M0 (0.62 mm/min^{0.5}). The improvement can be ascribed to GO's capability to refine the pore structure of the cement matrix and decrease the connectivity of capillary pores, thus restricting water absorption through capillary action [22].

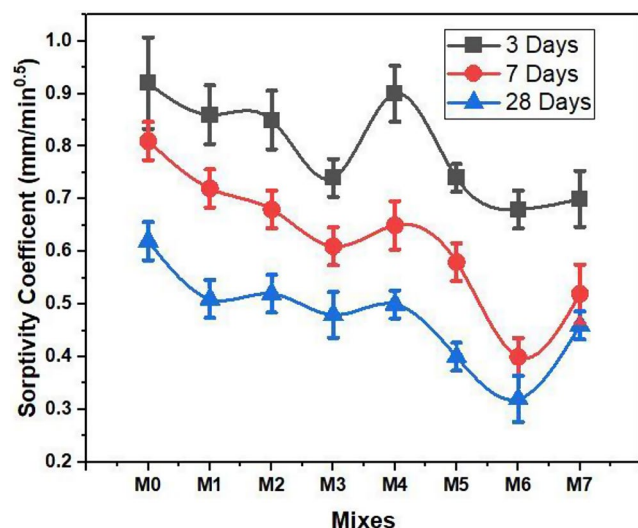


Fig. 13 Sorptivity coefficients for LC3

Among the LC3 mixes without GO (M2, M3, and M4), M3 with a 45:35 clinker to calcined clay ratio demonstrated the lowest sorptivity coefficient (0.48 mm/min^{0.5}), which is 29.16% lower than that of the reference mix (M0). The decrease in water absorption can be ascribed to the pozzolanic reaction of the calcined clay, which leads to the creation of supplementary hydration products that make the microstructure denser and reduce the porosity of the cement matrix [14].

The synergistic effect of combining GO and LC3 is evident from the remarkable reduction in the sorptivity coefficients of LC3 mixes containing 1% GO (M5, M6, and M7) compared to their corresponding LC3 mixes without GO. Mix M6 (LC3 with a 45:35 clinker to calcined clay ratio and 1% GO) exhibited the lowest sorptivity coefficient among all the investigated mixes, with a value of 0.32 mm/min^{0.5}, which is 93.75% lower than that of the reference mix (M0) and 59.37% lower than that of the normal concrete with 1% GO (M1). The substantial decrease in water absorption underscores the synergistic advantages of combining GO and LC3 to improve the durability of concrete.

The decrease in sorptivity coefficients of the LC3 mixtures containing GO can be ascribed to the combined effects of GO and calcined clay on the microstructure of the cement matrix. GO contributes to refining the pore structure and decreasing the connectivity of capillary pores, while the pozzolanic reaction of calcined clay results in the creation of supplementary hydration products that further densify the microstructure. This synergistic action produces a denser and less permeable cement matrix, which effectively impedes the ingress of water through capillary absorption.

3.7 Corrosion rate

Table 5 illustrates the corrosion rates of steel reinforcement embedded in various concrete mixes, including the reference mix (M0), normal concrete with 1% graphene oxide (GO) (M1), and limestone calcined clay cement (LC3) mixes with varying clinker to calcined clay ratios, both with and without GO addition. To assess the efficacy of the studied mixtures in shielding the steel reinforcement from corrosion, a critical factor in the durability of reinforced concrete structures [66], the corrosion rates were determined at various ages (3, 7, and 28 days).

The addition of 1% GO in normal concrete (M1) led to a substantial reduction in the corrosion rates compared to the reference mix (M0) at all ages. At 28 days, the corrosion rate of steel in M1 was 158.16 mm/year, which is 20.2% lower than that of M0 (198.32 mm/year). This enhancement can be attributed to GO's ability to refine the pore structure of the cement matrix, reducing the ingress of aggressive

Table 5 Corrosion rate

Mixes	Corrosion rate (mm/year)					
	3 Days	Std. deviation	7 Days	Std. deviation	28 Days	Std. deviation
M0	298.34	0.39128	264.31	0.34511	198.32	0.340441
M1	254.31	0.285832	185.34	0.44978	158.16	0.235797
M2	274.84	0.567098	202.74	0.57236	169.37	0.416773
M3	232.64	0.554256	184.61	0.34073	120.32	0.381576
M4	245.87	0.530189	194.37	0.38974	145.02	0.183303
M5	234.62	0.641561	174.31	0.46184	124.61	0.4996
M6	200.14	1.024305	142.84	0.51884	94.67	0.576888
M7	206.39	0.461303	165.37	0.38974	130.67	0.491223

agents like chloride ions and moisture, which are the primary contributors to steel corrosion [67].

Among the LC3 mixes without GO (M2, M3, and M4), M3 with a 45:35 clinker to calcined clay ratio demonstrated the lowest corrosion rates at all ages. At 28 days, the corrosion rate of steel in M3 was 120.32 mm/year, which is 39.3% lower than that of the reference mix (M0). The decrease in corrosion rates can be ascribed to the pozzolanic reaction of the calcined clay, which leads to the creation of supplementary hydration products that make the microstructure denser and reduce the porosity of the cement matrix, thus restricting the penetration of aggressive agents [62].

The synergistic effect of combining GO and LC3 is evident from the remarkable reduction in the corrosion rates of steel in LC3 mixes containing 1% GO (M5, M6, and M7) compared to their corresponding LC3 mixes without GO. Mix M6 (LC3 with a 45:35 clinker to calcined clay ratio and 1% GO) exhibited the lowest corrosion rates among all the investigated mixes at all ages. At 28 days, the corrosion rate of steel in M6 was 94.67 mm/year, which is 52.3% lower than that of the reference mix (M0) and 40.2% lower than that of the normal concrete with 1% GO (M1). The substantial decrease in corrosion rates underscores the synergistic advantages of combining GO and LC3 to improve the durability of reinforced concrete.

The decrease in corrosion rates of steel in the LC3 mixtures containing GO can be ascribed to the synergistic effects of GO and calcined clay on the microstructure of the cement matrix. GO contributes to refining the pore structure, decreasing the connectivity of capillary pores, and increasing the tortuosity of the pore network. Simultaneously, the pozzolanic reaction of calcined clay results in the creation of supplementary hydration products that further densify the microstructure [10, 64]. This synergistic action produces a denser and less permeable cement matrix, which effectively impedes the ingress of aggressive agents and offers improved protection to the embedded steel reinforcement.

These results underscore the significance of optimizing the mix design and utilizing advanced materials such as GO and LC3 to enhance the durability of reinforced concrete structures, consequently prolonging their service life and

minimizing maintenance costs related to corrosion-induced damage. Moreover, the standard deviations of the corrosion rates for each mix at different ages are relatively low, indicating the consistency and reliability of the experimental results. This consistency confirms the reproducibility of the corrosion resistance enhancement achieved by incorporating GO and LC3 in concrete mixes.

4 Conclusions

This study explored the impact of incorporating graphene oxide (GO) and optimizing the clinker to calcined clay ratio in limestone calcined clay cement (LC3) based concrete on “mechanical properties and durability performance”. The experimental results and analysis lead to the following conclusions:

- Incorporating 1% GO into conventional concrete (M1) considerably improved the “compressive strength, split tensile strength, and durability properties” compared to the reference mix (M0). The 28-day compressive strength and split tensile strength of M1 were 10.35% and 25.28% higher than those of M0, respectively. Adding GO also resulted in a significant decrease in “chloride ion penetration, water absorption, and corrosion rate of steel reinforcement”.
- Among the LC3 mixes without GO (M2, M3, and M4), M3 with a 45:35 clinker to calcined clay ratio demonstrated the best performance in terms of “mechanical properties and durability”. The 28-day compressive strength and split tensile strength of M3 were 4.69% and 5.63% higher than those of M2 (50:30 ratio), and 10.48% and 10.20% higher than those of M4 (40:40 ratio), respectively. M3 also exhibited the “lowest chloride ion penetration, water absorption, and corrosion rate” among the LC3 mixes without GO.
- The synergistic effect of combining GO and LC3 was evident from the remarkable improvement in the “mechanical properties and durability” of LC3 mixes containing 1% GO (M5, M6, and M7) compared to their

corresponding LC3 mixes without GO. Mix M6 (LC3 with a 45:35 clinker to calcined clay ratio and 1% GO) exhibited the best overall performance, with a 28-day compressive strength and split tensile strength of 52.39 MPa and 5.12 MPa, respectively, which were 27.40% and 45.45% higher than those of the reference mix (M0), and 15.44% and 16.09% higher than those of the normal concrete with 1% GO (M1). M6 also demonstrated the lowest “chloride ion penetration, water absorption, and corrosion rate” among all the investigated mixes.

- A strong positive correlation was observed between the “compressive strength and split tensile strength” of the concrete mixes, with a coefficient of determination (R^2) of 0.988. The relationship between these two mechanical properties can be expressed by the power function equation $CST = 0.0578(CS^{1.1347})$. The derived equation provided reliable predictions of the split tensile strength based on the compressive strength, with a mean absolute percentage error (MAPE) of 5.6%.
- The durability properties of the concrete mixes, including resistance to “chloride ion penetration, water absorption, and corrosion rate of steel reinforcement”, were significantly enhanced by the incorporation of GO and the optimization of the LC3 composition. The combined use of GO and LC3 resulted in a more compact and less permeable microstructure, which effectively hindered the ingress of aggressive agents and improved the overall durability performance of concrete.

In summary, the incorporation of GO and the optimization of the clinker to calcined clay ratio in LC3 based concrete led to significant improvements in mechanical properties and durability performance. The findings of this study highlight the potential of using GO and LC3 in combination to develop high-performance, sustainable, and durable concrete for various construction applications.

Author contributions Chava Venkatesh: writing original article, data analysis and experimental work Mallikarjuna. V: data analysis and supervisor G. Mallikarjuna Rao: data analysis and supervisor Santosh Kalyanrao Patil: Proof reading B.Naga kiran : Funding Yashwanth. M.K : editing and data visualization C. Venkata Siva Rama Prasad : Proof reading G. Sree Lakshmi Devi: Proof reading and data analysis.

Data availability No datasets were generated or analysed during the current study.

Declarations

Competing interests The authors declare no competing interests.

References

1. Miller SA, Horvath A, Monteiro PJ (2018) Impacts of booming concrete production on water resources worldwide. *Nat Sustain* 1(1):69–76. <https://doi.org/10.1038/s41893-017-0009-5>
2. Barbhuiya S, Nepal J, Das BB (2023) Properties, compatibility, environmental benefits and future directions of limestone calcined clay cement (LC3) concrete: a review. *J Building Eng* 107794. <https://doi.org/10.1016/j.jobbe.2023.107794>
3. Andrew RM (2018) Global CO₂ emissions from cement production, 1928–2017. *Earth Syst Sci Data* 10(4):2213–2239
4. Juenger MC, Snellings R, Bernal SA (2019) Supplementary cementitious materials: new sources, characterization, and performance insights. *Cem Concr Res* 122:257–273. <https://doi.org/10.1016/j.cemconres.2019.05.008>
5. Mañosa J, Calderón A, Salgado-Pizarro R, Maldonado-Alameda A, Chimenos JM (2024) Research evolution of limestone calcined clay cement (LC3), a promising low-carbon binder—A comprehensive overview. <https://doi.org/10.1016/j.heliyon.2024.e25117>. *Heliyon*
6. Scrivener K, Martirena F, Bishnoi S, Maity S (2018) Calcined clay limestone cements (LC3). *Cem Concr Res* 114:49–56. <https://doi.org/10.1016/j.cemconres.2017.08.017>
7. Al-Fakih A, Al-Shugaa MA, Al-Osta MA, Thomas BS (2023) Mechanical, environmental, and economic performance of engineered cementitious composite incorporated limestone calcined clay cement: a review. *J Building Eng* 107901. <https://doi.org/10.1016/j.jobbe.2023.107901>
8. Ferreira S, Herfort D, Damtoft JS (2017) Effect of raw clay type, fineness, water-to-cement ratio and fly ash addition on workability and strength performance of calcined clay–limestone Portland cements. *Cem Concr Res* 101:1–12. <https://doi.org/10.1016/j.cemconres.2017.08.003>
9. Rakhimova N (2024) Montmorillonite clays in Portland clinker-reduced, non-clinker cements, and cement composites: a review. *Constr Build Mater* 411:134678. <https://doi.org/10.1016/j.conbuildmat.2023.134678>
10. Cao Y, Wang Y, Zhang Z, Ma Y, Wang H (2021) Recent progress of utilization of activated kaolinitic clay in cementitious construction materials. *Compos Part B: Eng* 211:108636. <https://doi.org/10.1016/j.compositesb.2021.108636>
11. Ijaz N, Weimin YE, ur Rehman Z, Ijaz Z, Junaid MF (2023) Global insights into micro-macro mechanisms and environmental implications of limestone calcined clay cement (LC3) for sustainable construction applications. *Sci Total Environ* 167794. <https://doi.org/10.1016/j.scitotenv.2023.167794>
12. Avet F, Scrivener K (2018) Investigation of the calcined kaolinite content on the hydration of Limestone Calcined Clay Cement (LC3). *Cem Concr Res* 107:124–135. <https://doi.org/10.1016/j.cemconres.2018.02.016>
13. Krishnan S, Bishnoi S (2018) Understanding the hydration of dolomite in cementitious systems with reactive aluminosilicates such as calcined clay. *Cem Concr Res* 108:116–128. <https://doi.org/10.1016/j.cemconres.2018.03.010>
14. Dhandapani Y, Sakthivel T, Santhanam M, Gettu R, Pillai RG (2018) Mechanical properties and durability performance of concretes with Limestone Calcined Clay Cement (LC3). *Cem Concr Res* 107:136–151. <https://doi.org/10.1016/j.cemconres.2018.02.005>
15. Zunino F, Scrivener K (2022) Microstructural developments of limestone calcined clay cement (LC3) pastes after long-term (3 years) hydration. *Cem Concr Res* 153:106693. <https://doi.org/10.1016/j.cemconres.2021.106693>
16. Maraghechi H, Avet F, Wong H, Kamyab H, Scrivener K (2018) Performance of Limestone Calcined Clay Cement (LC 3) with

- various kaolinite contents with respect to chloride transport. *Mater Struct* 51:1–17. <https://doi.org/10.1617/s11527-018-1255-3>
17. Shi Z, Lothenbach B, Geiker MR, Kaufmann J, Leemann A, Ferreira S, Skibsted J (2016) Experimental studies and thermodynamic modeling of the carbonation of Portland cement, metakaolin and limestone mortars. *Cem Concr Res* 88:60–72. <https://doi.org/10.1016/j.cemconres.2016.06.006>
 18. Yang P, Dhandapani Y, Santhanam M, Neithalath N (2020) Simulation of chloride diffusion in fly ash and limestone-calcined clay cement (LC3) concretes and the influence of damage on service-life. *Cem Concr Res* 130:106010. <https://doi.org/10.1016/j.cemconres.2020.106010>
 19. Akarsh PK, Shrinidhi D, Marathe S, Bhat AK (2022) Graphene oxide as nano-material in developing sustainable concrete—A brief review. *Materials Today: Proceedings*, 60, 234–246. <https://doi.org/10.1016/j.matpr.2021.12.510>
 20. Zeng H, Qu S, Tian Y, Hu Y, Li Y (2023) Recent progress on graphene oxide for next-generation concrete: characterizations, applications and challenges. *J Building Eng* 69:106192. <https://doi.org/10.1016/j.jobe.2023.106192>
 21. Wu YY, Que L, Cui Z, Lambert P (2019) Physical properties of concrete containing graphene oxide nanosheets. *Materials* 12(10):1707. <https://doi.org/10.3390/ma12101707>
 22. Indukuri CSR, Nerella R, Madduru SRC (2019) Effect of graphene oxide on microstructure and strengthened properties of fly ash and silica fume based cement composites. *Constr Build Mater* 229:116863. <https://doi.org/10.1016/j.conbuildmat.2019.116863>
 23. Indukuri CSR, Nerella R (2021) Enhanced transport properties of graphene oxide based cement composite material. *J Building Eng* 37:102174. <https://doi.org/10.1016/j.jobe.2021.102174>
 24. Indukuri CSR, Nerella R, Madduru SRC (2020) Workability, microstructure, strength properties and durability properties of graphene oxide reinforced cement paste. *Australian J Civil Eng* 18(1):73–81. <https://doi.org/10.1080/14488353.2020.1721952>
 25. Devi SC, Khan RA (2020) Effect of graphene oxide on mechanical and durability performance of concrete. *J Building Eng* 27:101007. <https://doi.org/10.1016/j.jobe.2019.101007>
 26. Peng H, Ge Y, Cai CS, Zhang Y, Liu Z (2019) Mechanical properties and microstructure of graphene oxide cement-based composites. *Constr Build Mater* 194:102–109. <https://doi.org/10.1016/j.conbuildmat.2018.10.234>
 27. Sharma S, Kothiyal NC (2015) Influence of graphene oxide as dispersed phase in cement mortar matrix in defining the crystal patterns of cement hydrates and its effect on mechanical, microstructural and crystallization properties. *RSC Adv* 5(65):52642–52657. <https://doi.org/10.1039/C5RA08078A>
 28. Reddy PVRK, Prasad DR (2022) Investigation on the impact of graphene oxide on microstructure and mechanical behaviour of concrete. *J Building Pathol Rehabilitation* 7(1):30. <https://doi.org/10.1007/s41024-022-00166-1>
 29. Mohammed A, Sanjayan JG, Duan WH, Nazari A (2015) Incorporating graphene oxide in cement composites: a study of transport properties. *Constr Build Mater* 84:341–347. <https://doi.org/10.1016/j.conbuildmat.2015.01.083>
 30. Reddy PVRK, Ravi Prasad D (2023) Graphene oxide reinforced cement concrete—a study on mechanical, durability and microstructure characteristics. *Fullerenes Nanotubes Carbon Nanostruct* 31(3):255–265. <https://doi.org/10.1080/1536383X.2022.2141231>
 31. He G, Yang C, Feng J, Wu J, Zhou L, Wen R, Xie X (2019) Hierarchical spiky microstraws-integrated microfluidic device for efficient capture and in situ manipulation of cancer cells. *Adv Funct Mater* 29(12):1806484
 32. Zhao L, Guo X, Song L, Song Y, Dai G, Liu J (2020) An intensive review on the role of graphene oxide in cement-based materials. *Constr Build Mater* 241:117939. <https://doi.org/10.1016/j.conbuildmat.2019.117939>
 33. Emmanuel AC, Haldar P, Maity S, Bishnoi S (2016) Second pilot production of limestone calcined clay cement in India: the experience. *Indian Concr J* 90(5):57–63
 34. Sharma M, Bishnoi S, Martirena F, Scrivener K (2021) Limestone calcined clay cement and concrete: a state-of-the-art review. *Cem Concr Res* 149:106564. <https://doi.org/10.1016/j.cemconres.2021.106564>
 35. Suo Y, Guo R, Xia H, Yang Y, Zhou B, Zhao Z (2022) A review of graphene oxide/cement composites: performance, functionality, mechanisms, and prospects. *J Building Eng* 53:104502. <https://doi.org/10.1016/j.jobe.2022.104502>
 36. Reddy PVRK, Prasad DR (2024) Nano-reinforced cement composites and novel insights from graphene oxide: a review. *Bull Mater Sci* 47(1):1–13. <https://doi.org/10.1007/s12034-023-03092-1>
 37. BIS IS 12269–2013 standards for ordinary Portland Cement, 53 Grade-specifications. Bureau of Indian Standards, New Delhi
 38. Zaaba NI, Foo KL, Hashim U, Tan SJ, Liu WW, Voon CH (2017) Synthesis of graphene oxide using modified hummers method: solvent influence. *Procedia Eng* 184:469–477. <https://doi.org/10.1016/j.proeng.2017.04.118>
 39. BIS, IS 383–2016 (2016) Specification for coarse and fine aggregates from natural sources for concrete. Bureau of Indian Standards, New Delhi
 40. BIS, IS 10262–2019 (2019) Specification for concrete mix proportioning. Bureau of Indian Standards, New Delhi
 41. BIS IS (2013) Specification for method of tests for concrete. Bureau of Indian Standards, New Delhi, pp 516–2013
 42. ASTM C192/C192M-19 Standard Practice for Making and curing concrete test specimens in the Laboratory. ASTM International, West Conshohocken, PA 19428–2959. United States.
 43. ASTM C39/C39M-20 Standard test method for compressive strength of cylindrical concrete specimens. ASTM International, West Conshohocken, PA 19428–2959. United States.
 44. ASTM C496/C496M-17 Standard Test Method for Splitting Tensile Strength of Cylindrical concrete specimens. ASTM International, West Conshohocken, PA 19428–2959. United States.
 45. ASTM C1202-19 (2019) Standard test method for electrical indication of concrete’s ability to resist chloride ion penetration. ASTM International, West Conshohocken, PA
 46. NT Build 492 Standard Test Method for Chloride Migration Coefficient from Non-Steady-State Migration Experiments
 47. ASTM C1585-13 Standard Test Method for Measurement of Rate of Absorption of Water by hydraulic-cement concretes. ASTM International, West Conshohocken, PA 19428–2959. United States.
 48. ASTM G59-97 (2020) Standard test method for conducting potentiodynamic polarization resistance measurements. ASTM International, West Conshohocken, PA
 49. Maxwell SE, Delaney HD, Kelley K (2018) Designing experiments and analyzing data: a model comparison perspective, 3rd edn. Routledge
 50. Lu Z, Hou D, Meng L, Sun G, Lu C, Li Z (2015) Mechanism of cement paste reinforced by graphene oxide/carbon nanotubes composites with enhanced mechanical properties. *RSC Adv* 5(122):100598–100605. <https://doi.org/10.1039/C5RA18602A>
 51. Satdive A, Tayde S, Tonde S, Hazra C, Kundu D, Chatterjee A (2022) Bionanocomposites in the construction and building applications. *Polymer based bio-nanocomposites: Properties, durability and applications*. Springer Singapore, Singapore, pp 293–310. https://doi.org/10.1007/978-981-16-8578-1_16
 52. Neville AM (2011) Properties of concrete, 5th edn. Pearson Education Limited, Harlow
 53. Wang Q, Cui X, Wang J, Li S, Lv C, Dong Y (2017) Effect of fly ash on rheological properties of graphene oxide cement

- paste. *Constr Build Mater* 138:35–44. <https://doi.org/10.1016/j.conbuildmat.2017.01.126>
54. Tong T, Fan Z, Liu Q, Wang S, Tan S, Yu Q (2016) Investigation of the effects of graphene and graphene oxide nanoplatelets on the micro-and macro-properties of cementitious materials. *Constr Build Mater* 106:102–114. <https://doi.org/10.1016/j.conbuildmat.2015.12.092>
55. Wang Q, Wang J, Lu CX, Liu BW, Zhang K, Li CZ (2015) Influence of graphene oxide additions on the microstructure and mechanical strength of cement. *New Carbon Mater* 30(4):349–356. [https://doi.org/10.1016/S1872-5805\(15\)60194-9](https://doi.org/10.1016/S1872-5805(15)60194-9)
56. Tironi A, Trezza MA, Scian AN, Irassar EF (2013) Assessment of pozzolanic activity of different calcined clays. *Cem Concr Compos* 37:319–327. <https://doi.org/10.1016/j.cemconcomp.2013.01.002>
57. Mehta PK, Monteiro PJ (2014) *Concrete: microstructure, properties, and materials*, 4th edn. McGraw-Hill Education, New York
58. CHAVA V, Rao S, MUNUGALA PK, CHEREDDY SSD (2024) Effect of mineral admixtures and curing regimes on properties of self-compacting concrete. *J Sustainable Constr Mater Technol* 9(1):25–35. <https://doi.org/10.47481/jscmt.1383493>
59. Ruben N, Venkatesh C, Durga CSS, Chand MSR (2021) Comprehensive study on performance of glass fibers-based concrete. *Innovative Infrastructure Solutions* 6(2):112. <https://doi.org/10.1007/s41062-021-00490-4>
60. Kumar R, Samui P, Rai B (2024) Prediction of the splitting Tensile Strength of Manufactured Sand based high-performance concrete using Explainable Machine Learning. *Iran J Sci Technol Trans Civil Eng* 1–18. <https://doi.org/10.1007/s40996-024-01401-0>
61. Angst UM (2018) Challenges and opportunities in corrosion of steel in concrete. *Mater Struct* 51(1):4. <https://doi.org/10.1617/s11527-017-1131-6>
62. Avet F, Snellings R, Diaz AA, Haha MB, Scrivener K (2016) Development of a new rapid, relevant and reliable (R3) test method to evaluate the pozzolanic reactivity of calcined kaolinitic clays. *Cem Concr Res* 85:1–11. <https://doi.org/10.1016/j.cemconres.2016.02.015>
63. Pillai RG, Gettu R, Santhanam M, Rengaraju S, Dhandapani Y, Rathnarajan S, Basavaraj AS (2019) Service life and life cycle assessment of reinforced concrete systems with limestone calcined clay cement (LC3). *Cem Concr Res* 118:111–119. <https://doi.org/10.1016/j.cemconres.2018.11.019>
64. Chougan M, Marotta E, Lamastra FR, Vivio F, Montesperelli G, Ianniruberto U, Bianco A (2019) A systematic study on EN-998-2 premixed mortars modified with graphene-based materials. *Constr Build Mater* 227:116701. <https://doi.org/10.1016/j.conbuildmat.2019.116701>
65. Venkatesh C, Nerella R, Chand MSR (2021) Role of red mud as a cementing material in concrete: a comprehensive study on durability behavior. *Innovative Infrastructure Solutions* 6(1):13. <https://doi.org/10.1007/s41062-020-00371-2>
66. Samson G, Deby F, Garcia JL, Lassoued M (2020) An alternative method to measure corrosion rate of reinforced concrete structures. *Cem Concr Compos* 112:103672. <https://doi.org/10.1016/j.cemconcomp.2020.103672>
67. Rezakhani D, Jafari AH, Hajabassi M (2023), March Durability, mechanical properties and rebar corrosion of slag-based cement concrete modified with graphene oxide. In *Structures* (Vol. 49, pp. 678–697). Elsevier. <https://doi.org/10.1016/j.istruc.2023.01.149>

Publisher's Note Springer Nature remains neutral with regard to jurisdictional claims in published maps and institutional affiliations.

Springer Nature or its licensor (e.g. a society or other partner) holds exclusive rights to this article under a publishing agreement with the author(s) or other rightsholder(s); author self-archiving of the accepted manuscript version of this article is solely governed by the terms of such publishing agreement and applicable law.